Mesomorphic Structures in Flexible Polymer−Surfactant Systems Due to Hydrogen Bonding: Poly(4-vinylpyridine)−Pentadecylphenol

Janne Ruokolainen, Gerrit ten Brinke,*,† and Olli Ikkala*

Department of Technical Physics, Helsinki University of Technology, Rakentajanaukio 2 C, FIN-02150 Espoo, Finland

Mika Torkkeli and Ritva Serimaa

Department of Physics, University of Helsinki, P.O. Box 9, FIN-00014 Helsinki, Finland

Received November 3, 1995; Revised Manuscript Received February 6, 1996[⊗]

ABSTRACT: Properly selected hydrogen bonding suffices to induce mesomorphic structures in mixtures of flexible polymers and nonmesogenic surfactants. For poly(4-vinylpyridine)−3-pentadecylphenol (P4VP-$(PDP)_x$) complexes, the long period of the lamellar structure *decreases* as x^{-1} (x is the number of PDP molecules per P4VP repeat unit) in complete contrast to similar polyelectrolyte systems. Upon cooling from 80 °C to the room temperature, the long period gradually increases and levels off at around 30 °C at a value which is approximately 4 Å above the starting value. After an induction time, a structural transformation occurs in the highly complexed samples, due to the crystallization of the alkyl side chains. It is accompanied by a sudden decrease in the long period of approximately 5 Å. However, the structure is not stable and after an additional induction time both structures are present in the samples. Arguments to explain most of the observed phenomena will be given.

1. Introduction

In recent years, novel concepts have been introduced to achieve liquid crystalline polymeric structures[1] by ingenious application of amphiphilic surfactants, i.e. molecules with polar heads and less polar tails. The latter moieties may consist of long flexible alkyl groups, in which case the resulting structures resemble those of the familiar block copolymer systems[2] or the comb shape polymers.[3] Motivated by the work of Cao et al.[4] on lyotropic semirigid polyaniline−camphorsulfonic acid (PANI−CSA) complexes in *m*-cresol, Fredrickson[5] suggested that even in flexible polymers, the excluded volume repulsion of the alkyl tails of the surfactants might stiffen the polymer backbone to such an extent that nematic "bottle-brush" structures are formed in good solvent for the alkyl chains. The predictions were general, although later results[6] have suggested that in the particular PANI−CSA in *m*-cresol, the steric match of phenyl−phenyl and hydrogen bonding interactions, i.e. molecular recognition, plays a role.

Specific interactions in mesomorphic self-organized polymeric systems are currently studied by many groups.[7−21] Surfactant-induced mesomorphic structures have been described for semirigid polymers.[7−10] Antonietti et al. have studied mesomorphic polyelectrolyte−surfactant structures where the highly ionic and the nonpolar alkyl layers alternate.[11−13] In the case of poly(acrylic acid), also a cylindrical closed packing morphology was observed, where the ionic backbone chains are embedded in a continuous alkyl matrix. By using polyacids and tertiary amine surfactants, Tal'roze et al. have very recently shown that mesomorphic structures can be obtained by combining polyacids with suitable, molecularly matching surfactants.[14−16] Brandys and Bazuin[17,18] demonstrated mesomorphic structures in poly(4-vinylpyridine) mixtures with mesogenic biphenyl derivatives bearing carboxyl groups at one end.

Atactic poly(4-vinylpyridine) and poly(2-vinylpyridine), i.e. P4VP and P2VP, can be complexed with different types of amphiphilic surfactants to yield mesomorphic behavior.[20,21] Strong protonic acid (*p*-dodecylbenzenesulfonic acid, i.e. DBSA) can be used as a surfactant and a layered structure is observed with the long period 27−29 Å, depending on the protonation level.[20] Layered liquid crystalline structures were observed for up to ca. 50 w/w % of $P4VP(DBSA)_{1.0}$ dissolved in xylene, indicating stretching of P4VP chains upon addition of xylene, which is a good solvent for the alkyl chains. However, bottle brush structures were not observed. At the high protonation levels, poly(vinylpyridine) contains a substantial amount of bound positive charges; i.e. it is a polyelectrolyte. The charges, although screened by the oppositely charged counterions due to sulfonate anions, will still have a strong influence on the available polymer conformations. In the case of pure polyelectrolytes, i.e. in the absence of charge screening, the chains are expected to become strongly stretched and in the limit of dilute solution and infinite chain length, the chains are expected to behave as rigid rods.[22,23] Screening reduces the Coulombic interactions and thereby the amount of stretching.[24−26] In the case of pure ionomers, i.e. at a smaller concentration of charges, it leads to the formation of multiplets and clusters.[27−29] This latter aspect will be rather important at moderate levels of complexation in our case.

Surfactants which form metal coordination bonding with the aminic nitrogens of poly(vinylpyridines) also render mesomorphic structures, as has been shown for P4VP complexed with zinc dodecylbenzenesulfonate, i.e. $Zn(DBS)_2$.[21] In this case, the pyridine rings are not converted to charged pyridinium rings. Note that there are no covalently *bound* charges along the polymer backbone, although there are still ionic charges *complexed* to the polymer because of the ionic zinc sulfonate

†Also: Laboratory of Polymer Chemistry and Materials Science Center, University of Groningen, Nijenborgh 4, 9747 AG Groningen, The Netherlands.

[⊗] Abstract published in *Advance ACS Abstracts,* April 1, 1996.

S0024-9297(95)01650-0 CCC: $12.00

salt of the surfactant. Therefore, the complications associated with the role of charges are still with us.

In this article we investigate mesomorphic structures of a flexible polymer, i.e. P4VP, which is hydrogen bonded to a nonmesogenic surfactant, i.e. 3-pentadecylphenol. In this case there are no ionic charges present. The expected requirement is that the interaction between the surfactant and the polymer is sufficiently strong. Then, the mesomorphic layered structures originate from microphase separation between the nonpolar surfactant tail layer and the polar polymer layer to which the surfactants are attached. These microphase-separated structures are in many respects, but not all, similar to those found in the familiar block copolymer systems. Some results have also been verified with poly(2-vinylpyridine) to confirm that the results are in no way related to the relatively high $T_g \approx 148$ °C of P4VP, compared to $T_g \approx 102$ °C for P2VP.

2. Experimental Section

Materials. The atactic P4VP and atactic P2VP were acquired from Polyscience Europe GmbH. The molar masses of P4VP ($M_v = 49\,000$ g/mol) and P2VP ($M_v = 330\,000$ g/mol) were determined by viscometry in absolute ethanol using $[\eta] = 2.5 \times 10^{-4} M_w^{0.68}$ [30] and DMF using $[\eta] = 1.47 \times 10^{-4} M_w^{0.67}$,[31] respectively. 3-Pentadecylphenol (PDP) was purchased from Aldrich. Ethanol and DMF were of analysis grade. All solvents were carefully dried by 3 Å molecular sieves.

Sample Preparation. P4VP and P2VP were first dried at 60 °C in vacuum for 2 days. Also PDP was dried at 60 °C in vacuum at least for 1 day. P4VP(PDP)$_x$ and P2VP(PDP)$_x$ complexes were prepared from DMF solutions. Here x denotes the number of surfactant molecules per vinylpyridine repeat unit. In each case, the surfactant and the solvent were first mixed together until a clear solution was obtained. P4VP or P2VP was subsequently added, followed by mechanical stirring for approximately 1 h at 60 °C. It was checked that the solutions had become clear. The concentrations were kept low (less than 2.5 w/w %) to ensure homogeneous complex formation. DMF was first evaporated on a hot plate at 70 °C. The complexes were further dried at 60 °C in vacuum at least for 2 days and thereafter stored in a desiccator. Samples for small angle X-ray measurements were annealed for 5 min at 180 °C to erase thermal history.

Small Angle X-ray Scattering. The SAXS method was used to analyze the mesomorphic behavior. The Cu Kα radiation was monochromatized by means of the combined action of a Ni filter and a totally reflecting mirror (Huber small angle chamber 701). The sealed Cu anode fine focus X-ray tube was powered by a Siemens Kristalloflex 710 H. The scattered radiation was detected by a linear one-dimensional position sensitive proportional counter (MBraun OED-50M). A narrow slit was used before the sample to minimize the background scattering. The primary beam is narrow (the full width at half-maximum FWHM < 0.002 Å^{-1}) compared to its length (FWHM = 0.027 Å^{-1}) at the sample. Together with the detector height profile, the FWHM of the instrumental function was 0.048 Å^{-1}. The smallest achievable k is only ca. 0.02 Å^{-1} by using this setup. The results have been plotted by using the wave vector $k = (4\pi/\lambda) \sin\theta$ where $\lambda = 1.542$ Å and 2θ is the scattering angle.

Wide Angle X-ray Scattering. The samples were pressed pellets with a thickness of 1 mm and a diameter of 20 mm. The temperature was 25 °C and two-circle diffractometers were used in a symmetrical transmission mode. The measurements were made with Cu Kα ($\lambda = 1.542$ Å) radiation monochromatized with a diffracted beam monochromator (graphite). The intensity curves were measured with a scintillation counter. The samples were in normal atmosphere and the air scattering was not subtracted. The scattering vector k was calculated as in SAXS.

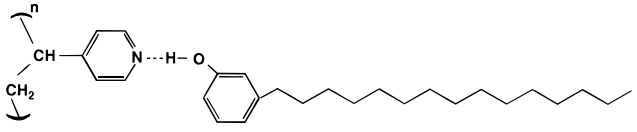

Figure 1. Hydrogen bond between poly(4-vinylpyridine) and pentadecylphenol.

Infrared Spectroscopy. Infrared spectra were obtained using a Nicolet 730 FTIR spectrometer. P4VP(PDP)$_x$ and pure PDP were prepared by melting directly onto potassium bromide crystals. Pure P4VP was dissolved in DMF and cast onto a potassium bromide crystal followed by evaporation at 80 °C and drying in vacuum at 60 °C for several hours. Overnight drying was required to remove remainders of DMF.

3. Results and Discussion

Infrared Spectroscopy. FT-IR was performed to study the complex formation between P4VP and PDP. Figure 1 presents a schematic picture of the complexation. Infrared spectroscopy is a powerful tool for the study of specific interactions in polymer blends[32] and in polymer−surfactant systems.[20,21] FT-IR features of interest have been considered recently in relation to polymer blends of P4VP and P2VP with other polymers containing hydroxyl groups that form hydrogen bonds with the basic nitrogen.[33−35] Studies of infrared spectra of pyridine hydrogen bonded with alcohols[36] and of interpolymer P2VP/poly(ethylene-*co*-methacrylic acid) complexes[37] demonstrate that the most affected bands of poly(vinylpyridines) are those concerned with the stretching modes of the pyridine ring: 1590, 993, and 625 cm^{-1} for P2VP and 1597, 993, and 627 cm^{-1} for P4VP. Upon formation of hydrogen bonding, these bands shift to higher frequencies. This effect is a consequence of changes in the electronic distributions in the pyridine ring due to the formation of stronger bonds. In our previous studies, similar but much larger band shifts were observed in the poly(vinylpyridine) complexes with a strong protonic acid[20] and in a metal coordination complex.[21] Figure 2 presents the FT-IR spectra of P4VP(PDP)$_x$ with surfactant mole fraction x = 0.25, 0.5, 0.75, and 1.0. The spectra of pure P4VP and pure PDP are given in the same picture. The most affected bands are presented in more detail in Figures 3 and 4. Figure 3 shows the spectra of the 1600 cm^{-1} region. Pure P4VP has an absorption band at 1597 cm^{-1}, and this band shifts to 1603 cm^{-1} upon formation of hydrogen bonds. Cesteros et al.[33−35] have observed exactly the same shifts in P4VP blends with polymers containing hydroxyl groups. Note, however, that it is very difficult to determine the actual degree of complexation based on these particular data, due to the nearby absorption peaks of pure PDP. Figure 3 presents also the region near the pure P4VP absorption band at 1415 cm^{-1}. This band should shift approximately +5 cm^{-1} on formation of a hydrogen bond.[36] This shift is now clearly observed because there is no

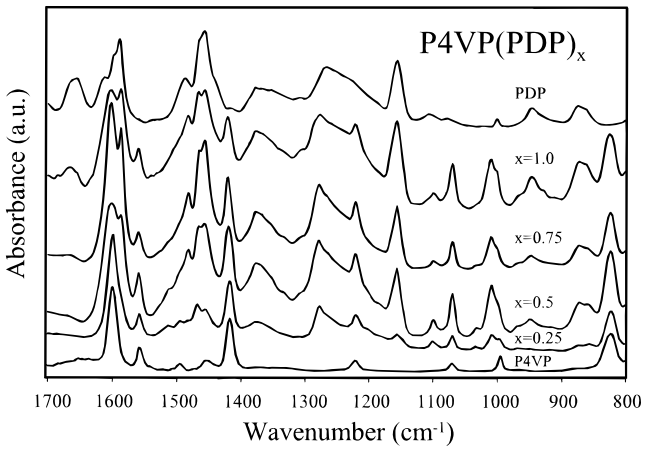

Figure 2. Infrared spectra of P4VP, PDP, and P4VP(PDP)$_x$ (x = 0.25, 0.5, 0.75, 1.0).

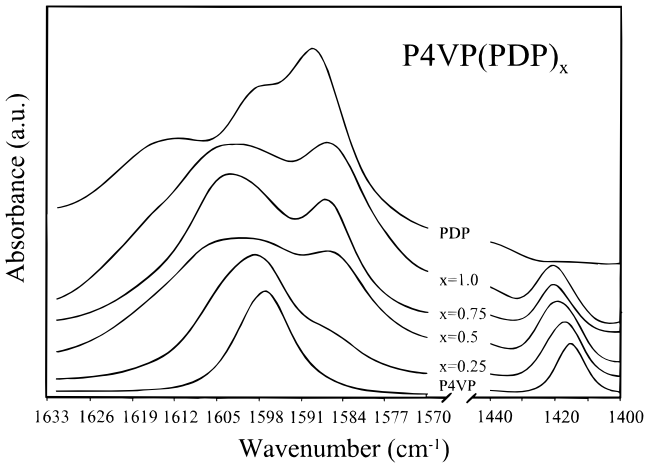

Figure 3. Infrared spectra in the 1400−1630 cm^{-1} region; same samples as Figure 2.

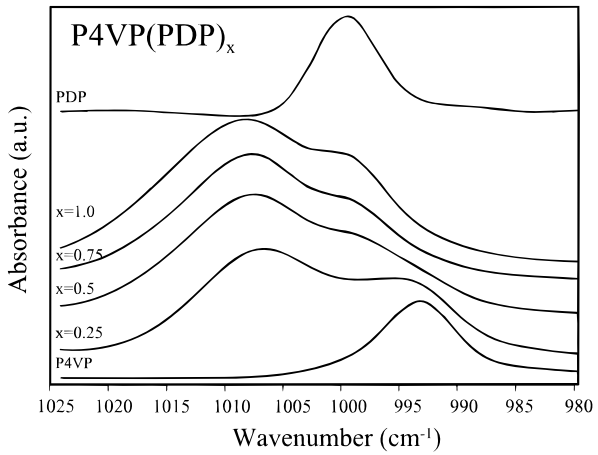

Figure 4. Infrared spectra in the 980−1025 cm^{-1} region; same samples as Figure 2.

overlapping absorption of pure PDP. For the nominally fully complexed case this peak is observed to shift to 1421 cm^{-1}. Figure 4 presents the spectra of the 1020−980 cm^{-1} region. The pure polymer has an absorption band at 993 cm^{-1} which shifts to 1008 cm^{-1} when the complex is formed. The free pyridine ring absorption band has vanished in the nominally fully complexed case. The phenyl ring of PDP creates a band near 1000 cm^{-1} which, however, is sufficiently far from the free pyridine ring absorption. The shifts related to the 1415 and 993 cm^{-1} bands indicate that the complex formation

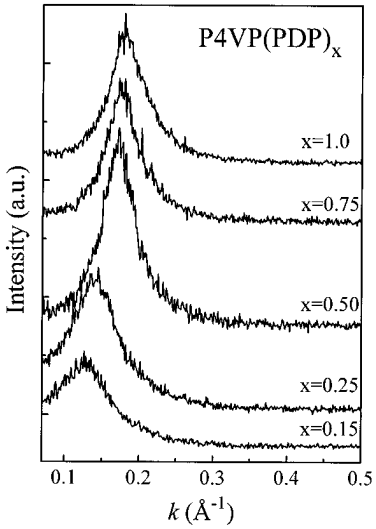

Figure 5. SAXS data for P4VP(PDP)$_x$ at 80 °C.

is essentially complete because in P4VP(PDP)$_{1.0}$ the absorption band due to the stretching vibration of the free P4VP ring has disappeared.

When the hydrogen bond is formed between the phenolic surfactant and the amine of the pyridine ring, the observed absorption band shift is relatively small; i.e. the pyridine band at 1597 cm^{-1} is observed to shift only +6 cm^{-1}. In the case of protonation or coordination bonding, the corresponding shifts were observed to be +40 and +20 cm^{-1}, correspondingly.[20,21] This indicates a much weaker interaction in the present case. In the next paragraph we will observe that the hydrogen bonding between PDP and P4VP is still strong enough to establish mesomorphic behavior. It is well-known that the strength of the hydrogen bond varies between different hydrogen bonding species, and in a future paper we will address this issue in more detail and establish that indeed a minimum strength is required.[38]

Small Angle X-ray Scattering. As usual, mesomorphic structures are most conveniently investigated using SAXS. Figure 5 shows the SAXS intensity curves obtained at 80 °C. This temperature has the advantage that most of the P4VP(PDP)$_x$ samples, except for very small values of x, are in the (highly viscous) melt state. All curves, as well as those taken at 22 °C, show distinct diffraction maxima, which shift to *larger* angles for increasing values of x. The latter observation came to us as a great surprise because previously we observed the diffraction maxima to shift to *smaller* angles for P4VP(DBSA)$_x$ and P4VP(Zn(DBS)$_2$)$_x$, though with a much weaker x dependence.[20,21] Figure 6 presents the long period as a function of x, together with fits based on a $1/x$ behavior. The fits are remarkably good. Figure 7 depicts potential structures that are able to explain the observed SAXS behavior. Figure 7a shows the case where x = 0.25 where the surfactants are uniformly distributed along the polymer backbone, leading to thick polar layers. In this schematic picture, the opposite surfactant layers do not interpenetrate and the surfactant molecules are uniformly stretched. In reality, a slight interpenetration will be present[39−41] and the end points will be distributed throughout the layer,[42,43] but this is of no consequence for the following argument. The essential element is the assumption that the stretching of the surfactant tails is approximately independent of x, whereas the thickness of the polymer layer decreases accordingly for increasing x. A

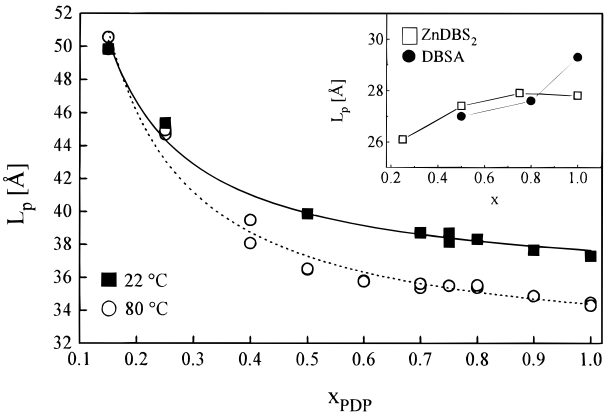

Figure 6. Long period as a function of x for P4VP(PDP)$_x$ at 80 °C and at room temperature. The curves are $1/x$ fits. Inset: long period of P4VP(DBSA)$_x$[20] and P4VP(Zn(DBS)$_2$)$_x$,[21] both at room temperature.

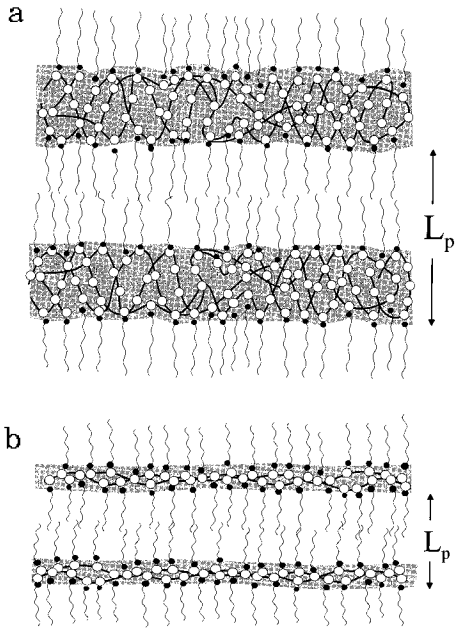

Figure 7. Schematic structure of P4VP(PDP)$_x$: (a) $x = 0.25$; (b) $x = 1.0$.

simple geometric argument then gives

$$L_p \propto 1/x \tag{1}$$

The free energy of this model consists of contributions due to the confinement of the polymer molecules in a two-dimensional layer, the stretching of the surfactant side chains attached to this layer, and the interfacial interactions. A simple analysis demonstrates that for a range of x values this picture is essentially correct.[44]

The lamellar structure proposed has many features in common with the microphase-separated state of block copolymers, and it is of some interest to discuss this structure in terms of the familiar block copolymer concepts. The classical ordered structures in block copolymer systems are lamellar, cylindrical, and spherical, but recently, various bicontinuous structures have been reported as well.[2] We will restrict ourselves to the three classical structures and base our discussion on arguments first given by Semenov.[45] In our case, x determines the volume fraction f of the surfactant material. For block copolymers, f is the essential parameter with respect to the mesomorphic structures. For a given value of f, the different classical morphologies all represent a similar level of stretching of the chain molecules involved. The essential difference is the interfacial area, which, therefore, determines to a large extent the final equilibrium structure. Consider a cubic piece of the material with dimensions equal to the long period L_p. The corresponding interfacial areas for the lamellar, cylindrical, and spherical morphologies are given by[45] $2L_p^2$, $2L_p^2(\pi f)^{1/2}$, and $L_p^2(36\pi)^{1/3}f^{2/3}$, respectively. Since it is primarily the amount of the interface material that determines the morphology, the structure with the smallest interfacial area being the stable one, these expressions imply that to a good approximation, the various structures occur for f values as follows: *lamellar*, $0.32 \le f \le 0.68$; *cylindrical*, $0.16 \le f \le 0.32$ and $0.68 \le f \le 0.84$; and *spherical*, $f \le 0.16$ and $f \ge 0.84$. The exact results for diblock copolymers differ slightly from these,[2] but since in our case we are dealing with a different situation consisting of a combination of stretching and confining, they would not necessarily be a better estimate. In the case of P4VP(PDP)$_x$, we can assume that the surfactant layer comprises either all surfactant molecules or only the alkyl chains. We will consider both possibilities separately.

In the first case, the volume fraction of the surfactant layer f can be estimated as $f = 303x/(303x + 105)$ on the basis of the molecular weights of 105 for a repeat unit of P4VP and 303 for the surfactant molecule PDP (ignoring the "shared" proton) and by ignoring any difference in density. In this case we obtain

$$\textit{spherical}: \; x \le 0.066 \tag{2}$$

$$\textit{cylindrical}: \; 0.066 \le x \le 0.16 \text{ and } x \ge 0.74 \tag{3}$$

$$\textit{lamellar}: \; 0.16 \le x \le 0.74 \tag{4}$$

These results imply that a lamellar morphology is highly favored for the P4VP(PDP)$_x$ system. However, the highly complexed cases are then predicted to be cylindrical (or more complicated). Our SAXS data show no evidence for cylindrical structures. We do observe additional WAXS peaks at room temperature; however, as will be discussed, these are due to the crystallization of the alkyl chains. On the other hand, Antonietti et al.[12] reports to have found cylindrical structures in fully complexed poly(acrylic acid)−dodecyltrimethylammonium systems.

In the second case, if we assume that the surfactant layer consists of the alkyl chain material only, and now take the difference between the density of the pure alkyl layer (≈0.9 g cm^{-3}) and the highly polar layer (≈1.2 g cm^{-3}) into account, we find in a similar way using $f = 211x/(211x+148)$:

$$\textit{spherical}: \; x \le 0.12 \tag{5}$$

$$\textit{cylindrical}: \; 0.12 \le x \le 0.33 \tag{6}$$

$$\textit{lamellar}: \; x \ge 0.33 \tag{7}$$

Since the most unfavorable interactions are likely those between the polar material, including the polymer and the phenol group, and the nonpolar alkyl chains, the second possibility seems most reasonable. It predicts that at relatively low values of complexation, a transition from the lamellar structure to a different structure should occur. So far we have found no signs of it in our systems, however, the signals at small values of x being rather weak. Moreover, the fact that the polymer−surfactant complexes resemble more closely

comb shape copolymers, even though polymer and surfactant are not covalently bound, sets these systems apart from the conventional block copolymer systems. Antonietti et al.[11−13] for instance also observed a preference for lamellar structures in polyelectrolyte systems. A series of complexes between poly(styrenesulfonate) and alkyltrimethylammonium counterions (C_{12}−C_{18}) are reported to exhibit a principal lamellar morphology. Only for the longest surfactants are the undulations of the interface large enough to localize a face-centered cubic (fcc) arrangement but still within a lamellar morphology. Also, Tal'roze et al.[14−16] found lamellar structures in their polyacid−amine systems.

Being able to understand the $1/x$ dependence of the long period in the case of P4VP(PDP)$_x$, the next issue is the opposite behavior of the previously studied P4VP(DBSA)$_x$ and P4VP(Zn(DBS)$_2$)$_x$ systems. Figure 6 also shows the long period of these systems as a function of x.[20,21] The data are obtained at room temperature, which in this case makes no difference, since, in contrast to the P4VP(PDP)$_x$ systems, crystallization of the shorter dodecyl alkyl tails was not observed. This different behavior of the long period must clearly be related to the nature of the polymer−surfactant interactions. Hydrogen bonds have interaction strengths of the order of 1−8 kcal mol^{-1}, and such low energies imply a very dynamic situation where the bonds are continuously reformed and broken. For the previously considered systems, P4VP(DBSA) and P4VP(Zn(DBS)$_2$), the interaction energies are much higher but, what is perhaps more important, in both these cases charges are involved. A considerable fraction of these systems consists of nonpolar alkyl chains, and for not too large values of x, we are actually dealing with ionomers for which a huge amount of information is available (cf. reviews, refs 27−29). Although many issues have not really been settled, the current view is that in conventional ionomers, the ionic species aggregate at two different levels, multiplets and clusters. Multiplets are considered to consist of small numbers of associated ion pairs in spherical ionic domains. Lamellar domains, which do not restrict the number of ion pairs present, have also been suggested. In the P4VP(DBSA)$_x$ and P4VP(Zn(DBS)$_2$)$_x$ systems, the electrostatic interactions are expected to be important, as in ionomers. Because steric hindrance becomes even more of a problem in the case of long surfactant molecules, and because, in principle, every pyridine group is available for complexation, we propose that the surfactant molecules will in fact cluster together along the chains in a manner as illustrated in Figure 8. This clustering may already happen during the complexation, since it is known that polyelectrolyte−surfactant complexation occurs in a highly cooperative manner.[46−47] Alternatively, it might take place in the liquid state after complexation in solution during annealing, due to a rearrangement of the complexing sites. In this case, the packing constraints associated with the ionic clustering are apparently easier to satisfy. This model implies an almost constant long period as a function of x, with the slight increase observed experimentally due to a diminishing influence of the domain boundaries. Further evidence based on WAXS and SAXS on this type of clustering has been recently reported for mesomorphic complexes of nylon 6 with Zn(DBS)$_2$.[48]

Finally, we want to stress that Figures 7 and 8 are intended only to illustrate the possible surfactant aggregation and its effect on the measured long period.

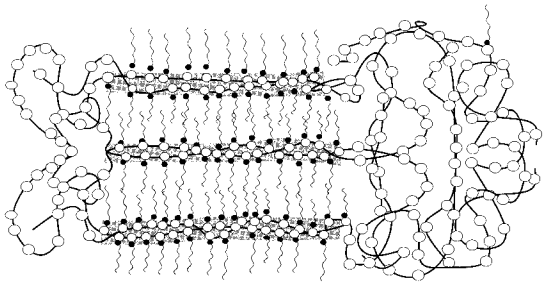

Figure 8. Schematic local structure in P4VP(DBSA)$_x$, due to the suggested cooperative complexation.

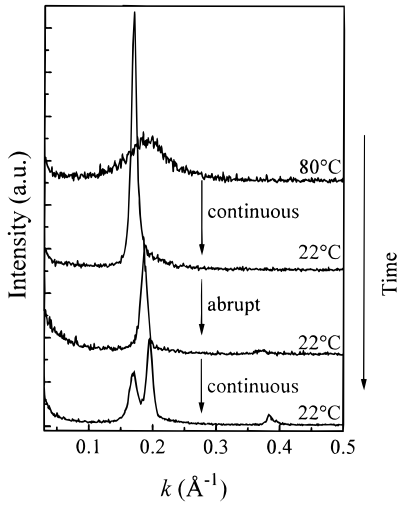

Figure 9. Sequence of SAXS intensity curves of P4VP(PDP)$_{1.0}$ as they develop during time.

Therefore, within this context it is not yet known whether the alkyl tails are in normal or tilted alignment relative to the polymer layers.

Small and Wide Angle X-ray Scattering. Morphology at Room Temperature. Figure 9 presents SAXS intensity curves of P4VP(PDP)$_{1.0}$ at 80 °C and at room temperature at different stages during a very slow cooling (<1 °C/min) from the initial temperature of 80 °C to the room temperature. The position of the SAXS peak gradually shifts to smaller angles until it levels off at ca. 30 °C at an angle corresponding to a long period of 38 Å, i.e. 4 Å above the starting value. During this cooling process, the SAXS peak intensity increases dramatically. We attribute this strongly increased order to the improved ordering of the alkyl chains that are now below the melting point of pure PDP (T_m = 55 °C) (see, however, Note Added in Proof). The second curve in Figure 9 corresponds to this situation. Subsequently, a structural transformation takes place at the room temperature and two new peaks replace the former one peak, as demonstrated by the third curve. These peaks are the first- and the second-order reflections of the 34 Å periodicity. The complete transformation to this new structure takes place at the room temperature quite suddenly after an induction time of 5−10 min. The transition is, as will be shown by WAXS next, due to the crystallization of the alkyl chains, and the behavior is, of course, typical for the nucleation-controlled processes. The crystallization may be accompanied by a partial overlap of the side chains.[3,49−51] This latter conclusion is a direct consequence of the long period observed (34 Å) and the length of the PDP molecules (≈23 Å) involved (cf. Figure 7). Surpringly, it turns out that the structure is not stable. After annealing for 20 h at room temperature, the lowest curve of Figure 9 was

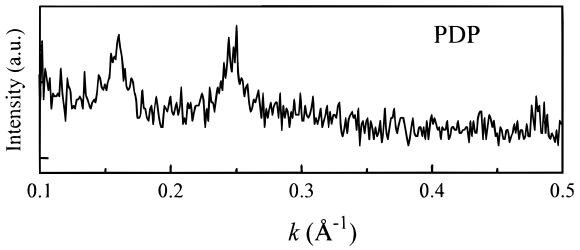

Figure 10. SAXS intensity curve for pure PDP at room temperature.

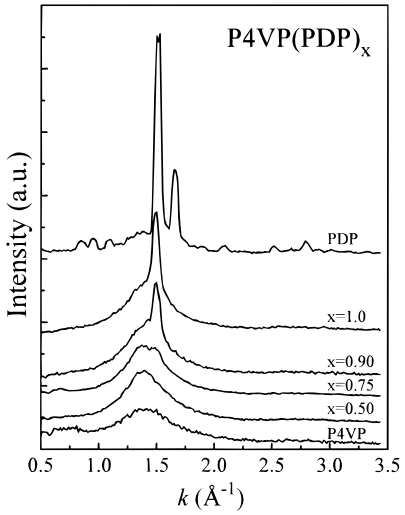

Figure 11. WAXS of pure PDP and P4VP(PDP)$_x$ at room temperature.

measured, now showing both structures to be present at the same time. So far, we have not come up with a satisfying explanation for this phenomenon. It definitely requires additional studies.

Figure 6 also presents the long period of all the P4VP(PDP)$_x$ samples as a function of x at room temperature corresponding to the amorphous structure, i.e. before the crystallization occurs. Within a reasonable time span, crystallization has only been observed in the samples with $x \geq 0.7$. This is most likely due to the limited mobility rather than the structure (cf. Figure 7). Pure P4VP has a glass transition temperature of 148 °C, and the mobility at the room temperature will greatly depend on the amount of the surfactant. The long periods of all the crystallized samples are around 34 Å, which is not surprising since the long periods of the highly complexed amorphous samples are also approximately the same. Figure 10 presents the SAXS intensity of pure PDP at the room temperature. PDP is crystalline under these conditions, and the sample contains two long periods at 39.4 and 25.4 Å. These presumably correspond to two different supramolecular structures involving a two-molecule and a one-molecule repeat, respectively. In all cases the dipoles will align in a thin layer. Clearly, the long periods in pure PDP are not directly related to the long periods in the crystallized P4VP(PDP) complexes.

Figure 11 presents the WAXS data for pure PDP and P4VP(PDP)$_x$. The precise crystal structures of PDP are not known yet. Nevertheless, the observed reflections at 4.20, 3.78, 3.05, 2.50, and 2.25 Å resemble closely those of comparable amphiphilic alkyl molecules and the strongest reflections correspond to the 110 and 200 reflections.[3,49−51] The WAXS of the complexes at moderate complexation shows an amorphous halo only, whereas at higher levels of complexation the original 110 reflection is prominently present. The second reflection has disappeared, however, indicating that the crystalline structure of the complex differs from that of pure PDP. These results correlate well with the SAXS data reported above.

4. Concluding Remarks

We observe that mesomorphic smectic like structures are created when flexible atactic polymer poly(4-vinylpyridine) is hydrogen bonded to a nonmesogenic surfactant, i.e. 3-pentadecylphenol. FTIR results suggest that essentially complete complexation of every pyridine ring is achieved. Astonishingly, at partial complexation the long period is observed to increase, in contrast to the previously reported charged polymer−surfactant complexes where it essentially remained constant. The difference is argued to be due to cooperative complexation in the latter case.

Strong segregation arguments demonstrate that, at least in our systems, the lamellar nature of the mesomorphic structures should prevail. One way of inducing different types of structures, such as cylindrical, is to use surfactant molecules with much longer alkyl tails.

Finally, the crystallization of the alkyl side chains gave rise to a striking new behavior. The crystallization of the highly complexed systems from the mesomorphic state is accompanied by a sudden reduction of the long period by more than 10%, which is attributed to an increased interdigitation between the opposite alkyl layers. This "collapse" has, as far as we know, not been observed before. Moreover, even more surprisingly, the crystallized systems turned out to be metastable. Again, it is of great interest to investigate similar systems, but with a different polymer and surfactant, to establish the general nature of these phenomena.

Acknowledgment. We acknowledge Maarit Taka of Neste Oy (Finland) for assistance in FT-IR measurements and Milja Karjalainen of Helsinki University for X-ray measurements. The work has been supported by the Finnish Academy, Technology Development Centre (Finland), and Neste Foundation.

Note Added in Proof. Time-resolved SAXS experiments have recently shown that the strong increase in scattering upon cooling corresponds to an order−disorder transition at ca. 60 °C. At elevated temperatures our samples appear to be in the homogeneous state. The strong segregation argument given to explain the 1/x behavior, therefore, only applies to the room temperature situation.[52]

References and Notes

(1) Weiss, R. A., Ober, C. K., Eds. *Liquid-Crystalline Polymers*; ACS Symposium Series No. 435; American Chemical Society: Washington, DC, **1990**.
(2) Bates, F. S.; Fredrickson, G. H. *Annu. Rev. Phys. Chem.* **1990**, *41*, 525.
(3) Platé, N. A.; Shibaev, V. P. *Comb-Shaped Polymers and Liquid Crystals*; Plenum Press: New York and London, 1987.
(4) Cao, Y.; Smith, P. *Polymer* **1993**, *34*, 3139.
(5) Fredrickson, G. H. *Macromolecules* **1993**, *26*, 2825.
(6) Ikkala, O. T.; Pietilä, L-O.; Ahjopalo, L.; Österholm, H.; Passiniemi, P. J. *J. Chem. Phys.* **1995**, *103*, 9855.
(7) Wernet, W.; Monkenbusch, M.; Wegner, G. *Makromol. Chem., Rapid Commun.* **1984**, *1*, 165.
(8) Wegner, G. *Makromol. Chem., Macromol. Symp.* **1986**, *1*, 151.
(9) Kärnä, T.; Laakso, J.; Savolainen, E.; Levon, K. European Patent Application EP 0 545 729 A1, **1993**.
(10) Levon, K.; Ho, K.-H.; Zheng, W.-Y.; Laakso, J.; Kärnä, T.; Taka, T.; Österholm, J.-E. *Polymer* **1995**, *36*, 2733.

(11) Antonietti, M.; Conrad, J.; Thünemann, A. *Macromolecules* **1994**, *27*, 6007.
(12) Antonietti, M.; Conrad, J. *Angew. Chem., Int. Ed. Engl.* **1994**, *33*, 1869.
(13) Antonietti, M.; Burger, C.; Effing, J. *Adv. Mater.* **1995**, *7*, 750.
(14) Tal'roze, R. V.; Platé, N. A. *Polym. Sci.* **1994**, *36*, 1479 (translated from *Vysokomol. Soedin.* **1994**, *36*, 1766).
(15) Tal'roze, R. V.; Kuptsov, S. A.; Sycheva, T. I.; Shandryuk, G. A.; Platé, N.A. *Polym. Mater. Sci. Eng.* **1995**, *72*, 431.
(16) Tal'roze, R. V.; Kuptsov, S. A.; Sycheva, T. I.; Bezborodov, V. S.; Platé, N. A. *Macromolecules* **1995**, *28*, 8689.
(17) Brandys, F. A.; Bazuin, C. G. *Polym. Prepr.* (*Am. Chem. Soc., Div. Polym. Chem.*) **1993**, *34* (1), 186.
(18) Brandys, F. A.; Bazuin, C. G. *Chem. Mater.* **1992**, *4*, 970.
(19) Paleos, C. M.; Tsiourvas, D. *Angew. Chem., Int. Ed. Engl.* **1995**, *34*, 1696.
(20) Ikkala, O. T.; Ruokolainen, J.; ten Brinke, G.; Torkkeli, M.; Serimaa, R. *Macromolecules* **1995**, *28*, 7088.
(21) Ruokolainen, J.; Ikkala, O. T.; ten Brinke, G.; Torkkeli, M.; Serimaa, R. *Macromolecules* **1995**, *28*, 7799.
(22) De Gennes, P.-G.; Pincus, P.; Velasco, R. M.; Brochard, F. *J. Phys. (Paris)* **1976**, *37*, 1461.
(23) Pfeuty, P. *J. Phys. (Paris)* **1978**, *39*, C2−149.
(24) Li, H.; Witten, T. A. *Macromolecules* **1995**, *28*, 5921.
(25) Stevens, M. J.; Kremer, K. *Macromolecules* **1993**, *26*, 4717.
(26) Förster, S.; Schmidt, M.; Antonietti, M. *J. Phys. Chem.* **1992**, *96*, 4008.
(27) Eisenberg, A., Ed. *Ions in Polymers*; ACS Advances in Chemistry Series No. 187; American Chemical Society: Washington, DC, 1980.
(28) MacKnight, W. J.; Earnest, T. R. *J. Macromol. Sci. Rev.* **1981**, *16*, 41.
(29) Fitzgerald, J. J.; Weiss, R. A. *Rev. Macromol. Chem. Phys.* **1988**, *C28*, 99.
(30) Berkowitz, J. B.; Yamin, M.; Fuoss, R. M. *J. Polym. Sci.* **1958**, *28*, 69.
(31) Arichi, S. *Bull. Chem. Soc. Jpn.* **1966**, *39*, 439.
(32) Coleman, M. M.; Graf, J. F.; Painter, P. C. *Specific Interactions and the Miscibility of Polymer Blends*; Technomic: Lancaster, PA, 1991.
(33) Cesteros, L. C.; Meaurio, E.; Katime, I. *Macromolecules* **1993**, *26*, 2323.
(34) Cesteros, L. C.; Isasi, J. R.; Katime, I. *Macromolecules* **1993**, *26*, 7256.
(35) Cesteros, L. C.; José, L.;Katime, I. *Polymer* **1995**, *36*, 3183.
(36) Takahashi, H.; Mamola, K.; Plyler, E. K. *J. Mol. Spectrosc.* **1966**, *21*, 217.
(37) Lee, J. Y.; Painter, P. C.; Coleman, M. M. *Macromolecules* **1988**, *21*, 954.
(38) Ruokolainen, J.; Torkkeli, M.; Serimaa, R.; Vahvaselkä, S.; Saariaho, M.; Ten Brinke, G.; Ikkala, O. T. *Macromolecules*, submitted for publication.
(39) Zhulina, E. B.; Semenov, A. N. *Vysokomol. Soedin. A* **1989**, *31*, 177.
(40) Witten, T. A.; Leibler, L.; Pincus, P. *Macromolecules* **1990**, *23*, 824.
(41) Semenov, A. N. *Macromolecules* **1992**, *25*, 4967.
(42) Semenov, A. N. *Sov. Phys. JETP* **1985**, *61*, 733.
(43) Milner, S. T.; Witten, T. A.; Cates, M. E. *Europhys. Lett.* **1988**, *5*, 413; *Macromolecules* **1988**, *21*, 2610.
(44) Ten Brinke, G.; Ruokolainen, J.; Ikkala O. T. *Europhys. Lett.*, submitted for publication.
(45) Semenov, A. N. Lecture Notes, Utrecht, 1993.
(46) Goddard, E. D. *Colloid Surf.* **1986**, *19*, 301.
(47) Hayagawa, K.; Kwak, J. C. *J. Phys. Chem.* **1982**, *86*, 3866; **1983**, *87*, 506.
(48) Ruokolainen, J.; Torkkeli, M.; Serimaa, R.; Hinkula, J.; Ten Brinke, G.; Ikkala, O. T. *Langmuir*, submitted for publication.
(49) Kaufman, H. S.; Sacher, A.; Alfrey, T., Jr.; Frankuchen, I. *J. Am. Chem. Soc.* **1948**, *76*, 6280.
(50) Chen, S. A.; Ni, J, M. *Macromolecules* **1992**, *25*, 6081.
(51) Hsu, W. P.; Levon, K.; Ho, K. S.; Myerson, A. S.; Kwei, T. K. *Macromolecules* **1993**, *26*, 1318.
(52) Ruokolainen, J.; Torkkeli, M.; Serimaa, R.; Komanschek, E.; Ikkala, O.; ten Brinke, G. To be published.

MA9516504